MATCH
Communications in Mathematical and in Computer Chemistry

MATCH Commun. Math. Comput. Chem. **94** (2025) 355–384
ISSN: 0340–6253
doi: 10.46793/match.94-2.355N

Nonlinear Dynamics of Fractional-Order Chaotic Chemical Reactor System Based on the Adomian Decomposition Method and Its Control via Adaptive Sliding Mode Control

Haneche Nabil[a,*], **Hamaizia Tayeb**[b]

[a] *Mathematical Modeling and Simulation Laboratory, Department of Mathematics, University of Mentouri Brothers, Constantine 25000, Algeria*

[b] *Department of Mathematics, University of Mentouri Brothers, Constantine 25000, Algeria*

nabil.haneche@doc.umc.edu.dz, el.tayyeb@umc.edu.dz

(Received July 9, 2024)

Abstract

In this paper, a fractional-order 3D chemical chaotic reactor system (FOCRCS) is presented. By applying the Adomian decomposition method, the numerical solution of the FOCRCS is derived. In addition, the chaotic dynamics of FOCRCS are investigated. Using powerful nonlinear tools such as phase plots, bifurcation diagrams, and spectral entropy, the chaotic behavior in the 3D FOCRCS is established. We established that the FOCRCS can display many chemically observed reactor states, including stable, periodic, and chaotic behaviors. The main goal in this research is to control chaotic dynamics in the FOCRCS. In order to achieve this objective, an adaptive sliding mode control is introduced. In addition, chaos synchronization scheme is presented to control chaotic dynamics in the studied chemical reactor system.

*Corresponding author.

1 Introduction

In recent years, the topic of chaotic systems has received great attention from a number of researchers in chaos theory [25]. The main reason for this interest is due to the many applications of chaotic systems in sciences and engineering. Biology [27], ecology [24], psychology [31], neural networks [19], cryptography [47, 49], lasers [38], memristors [42, 41], mechanics [6], chemistry [50], and secure communications [17, 46] are most fields were the chaotic systems are frequently applied in practice. A chaotic system is defined as dynamical system displays what is called sensitive dependence on initial conditions. A small change in initial state of chaotic system may lead to completely different outcomes [12]. In nonlinear dynamical analysis, a chaotic system has at least one positive Lyapunov exponent, in which the Lyapunov exponent is a numerical quantity that measure the rate of convergence and divergence of neighboring trajectories in nonlinear dynamical system [36].

Recently, fractional calculus becomes an important topic in mathematics and physics. Due to the hereditary and non-local distributed behaviors in dynamic phenomena, the modeling of systems in sciences and engineering by fractional differential equations is more suitable than integer-order equations [2]. Since the works of Leibniz in 1965, the idea of fractional derivative of continuous function has been explored [21]. In recent decades, many fractional differential and integral operators have been defined [15]. There are two kinds of fractional derivatives in the context of differential operators: those with singular kernels and those without. Well-known fractional derivatives with singular kernels are the Riemann-Liouville derivative and the Caputo derivative [22, 32]. Alternatively, without singular kernel, we have the fractional derivative with an exponential kernel, also referred to as the Caputo-Fabrizio fractional derivative [9], and the Atangana-Baleanu fractional derivative, which has a Mittag-Leffler kernel. Actually, due to their complexity, there are only three numerical methods to solve fractional-order chaotic systems numerically: frequency domain method (FDM) [10], Adams-Bashforth-Moulton method (ABM) [37], and Adomian decomposition method (ADM) [1]. Us-

ing ADM is more reasonable than the other two methods due to its precision, calculation speed, and low computer resources consumption [8]. In the current paper, based on previous advantages, the numerical solution of the fractional-order chemical system is investigated by employing ADM. The application of fractional calculus in modeling of physical and chemical systems has become widespread. In chemistry, authors in [20] have analyzed the chaotic behavior in 3D integer-order chaotic reactor system. Moreover, they have achieved chaos synchronization scheme to synchronize the chaotic states in the chemical reactor system. In [5], Bodale et al. have investigated the dynamics and chaos control for Willamowski-Rössler model of chemical reactors. In physics, several chaotic memristive systems have been extensively analyzed and controlled [33, 30].

Nowadays, control and synchronization of chaos phenomena in fractional-order physical and chemical chaotic systems have significant interest, as shown in the literature. The desired goal is to construct a suitable feedback control law to stabilize the state trajectories of the chaotic dynamical system [45]. Many control schemes have been introduced to control and synchronize fractional-order chaotic systems such as adaptive control [13], robust control [4], active control [51], sliding mode control [3], etc. In addition, the application of synchronization of chaotic systems in cryptography and secure communication schemes is studied in [52], [23] and [48].

The remainder of this paper is organized as follows. Basic tools of fractional calculus are introduced in Section (2). The numerical solution of the FOCRCS is derived using ADM algorithm is presented in Section (3). In Section (4), the stability of equilibria for the fractional-order chaotic system is analyzed. In section (5), varying the value of the fractional order and system parameters, the dynamics of the FOCRCS are analyzed via powerful tools such as phase plots, bifurcation diagrams, and spectral entropy. In Section (6), an adaptive sliding mode control method is presented to control chaotic motions in the FOCRCS. Moreover, a chaos synchronization scheme for the chemical system is constructed. We draw conclusions in Section (7).

2 Mathematical background

We give some basic notions of fractional calculus that will aid us in the rest of this paper.

Definition 1. The Riemann-Liouville fractional integral of order $q \in \mathbb{R}^+$ of a continuous function $u : \mathbb{R}^+ \to \mathbb{R}$ is defined as [16]

$$J_{t_0}^q u(t) = \frac{1}{\Gamma(q)} \int_{t_0}^{t} (t-s)^{q-1} u(s) ds, \tag{1}$$

where $t > t_0$, $\Gamma(.)$ represents the Gamma function.

For $\epsilon > -1$ and C is a given real constant, we have the following properties of the fractional integral operator $J_{t_0}^q$

$$\begin{aligned} &J_{t_0}^0 u(t) = u(t), \\ &J_{t_0}^q (t-t_0)^\epsilon = \frac{\Gamma(\epsilon+1)}{\Gamma(\epsilon+1+q)} (t-t_0)^{\epsilon+q}, \\ &J_{t_0}^q C = \frac{C}{\Gamma(q+1)} (t-t_0)^q, \end{aligned} \tag{2}$$

Definition 2. The Caputo fractional derivative of order $q \in \mathbb{R}^+$ of a continuous function $u : [t_0, +\infty[\to \mathbb{R}$ is defined as [29]

$${}^*D_{t_0}^q u(t) = \frac{1}{\Gamma(m-q)} \int_{t_0}^{t} \frac{u^{(m)}(s)}{(t-s)^{q+1-m}} ds, \tag{3}$$

where $t > t_0$, $m-1 < q \leq m$ with $m = \lceil q \rceil$.

We have the following two fundamental properties of the differential operator ${}^*D_{t_0}^q$:

$$\begin{aligned} {}^*D_{t_0}^q J_{t_0}^q u(t) &= u(t), \\ J_{t_0}^q ({}^*D_{t_0}^q) u(t) &= J_{t_0}^q J_{t_0}^{m-q} D_{t_0}^m u(t) \\ &= J_{t_0}^m D_{t_0}^m u(t) \\ &= u(t) - \sum_{n=0}^{m-1} u^{(n)}(t_0^+) \frac{(t-t_0)^n}{n!}. \end{aligned} \tag{4}$$

2.1 Adomian decomposition algorithm

A fractional-order nonlinear system can be divided into three parts as follows

$$ {}^{*}D^{q}_{t_0}u(t) = Lu(t) + Nu(t) + v(t), \tag{5} $$

where $u(t) = [u_1(t), u_2(t), \ldots, u_n(t)]^T$ is the system state variables where n is the system dimension. $Lu(t)$ and $Nu(t)$ are the linear and nonlinear terms in the fractional-order system respectively,
$v(t) = [v_1(t), v_2(t), \ldots, v_n(t)]^T$ is the constant term in the system and ${}^{*}D^{q}_{t_0}$ is the Caputo derivative operator with order q. The initial conditions are set as $u^{(k)}(t_0^+) = b_k = [u_1(t_0), u_2(t_0), \ldots, u_n(t_0)]^T, k = 0, 1, \ldots, m-1, m \in \mathbb{N}$, $m - 1 < q \leq m$. By applying the fractional integral operator $J^{q}_{t_0}$ to both sides of equation (28), we obtain [34]

$$ u(t) = J^{q}_{t_0}Lu(t) + J^{q}_{t_0}Nu(t) + J^{q}_{t_0}v(t) + \psi, \tag{6} $$

where $\psi = \sum_{k=0}^{m-1} b_k \frac{(t-t_0)^k}{k!}$. Employing the next recursive formulas

$$ \begin{aligned} u^0 &= \sum_{k=0}^{m-1} b_k \frac{(t-t_0)^k}{k!} + \psi, \\ u^1 &= J^{q}_{t_0}Lu^0 + J^{q}_{t_0}A^0(u^0), \\ u^2 &= J^{q}_{t_0}Lu^1 + J^{q}_{t_0}A^1(u^0, u^1), \\ &\vdots \\ u^i &= J^{q}_{t_0}Lu^{i-1} + J^{q}_{t_0}A^{i-1}(u^0, u^1, \ldots, u^{i-1}), \\ &\vdots \end{aligned} \tag{7} $$

Hence, the exact solution of the fractional-order system is obtained as

$$ u = \sum_{j=0}^{\infty} u^j = J^{q}_{t_0} \sum_{j=0}^{\infty} u^j + J^{q}_{t_0} \sum_{j=0}^{\infty} A^j + J^{q}_{t_0}u + \psi. \tag{8} $$

where A^j is the Adomian polynomial, which is expressed as [7]

$$A^j = \frac{1}{j!}\left[\frac{d^j}{d\lambda^j} N\left(\sigma_i^j(\lambda)\right)\right]_{\lambda=0}, \tag{9}$$

where $\sigma_i^j(\lambda) = \sum_{k=0}^{j}(\lambda)^k u_i^k$, $j = 0, 1, \ldots, \infty$ and $i = 1, 2, \ldots, n$.
We can evaluate the nonlinear part Nu of the fractional-order system by

$$Nu = \sum_{j=0}^{\infty} A^j(u^0, u^1, \ldots, u^j). \tag{10}$$

In practice, to obtain an approximate solution of Eq.(5), we only need to compute the first terms because the ADM algorithm converges quickly [44].

3 Fractional-order chaotic reactor model

In [43], Wang et al. established that the Lorenz equation can be transformed such that the original dynamic properties remain but the variables can only accept positive values. This transformation is described by the following relations

$$\begin{aligned}
&(R_1): X + Y + Z \xrightarrow{c_1} X + 2Z, \quad (R_2): A_1 + X + Y \xrightarrow{c_2} 2X + Y,\\
&(R_3): A_2 + X + Y \xrightarrow{c_3} X + 2Y, \quad (R_4): X + Z \xrightarrow{c_4} X + P_1,\\
&(R_5): Y + Z \xrightarrow{c_5} 2Y, \quad (R_6): 2X \xrightarrow{c_6} P_2,\\
&(R_7): 2Y \xrightarrow{c_7} P_3, \quad (R_8): 2Z \xrightarrow{c_8} P_4,\\
&(R_9): A_3 + X \xrightarrow{c_9} 2X, \quad (R_{10}): X \xrightarrow{c_{10}} P_5,\\
&(R_{11}): Y \xrightarrow{c_{11}} P_6, \quad (R_{12}): A_4 + Y \xrightarrow{c_{12}} 2Y,\\
&(R_{13}): A_5 + Z \xrightarrow{c_{13}} 2Z.
\end{aligned} \tag{11}$$

Assumed to be constant, the concentrations of species $A_j (j = 1, 2, \ldots, 5)$ and $P_j (j = 1, 2, \ldots, 6)$ have been included in the rate constants α_j. Based on these relations, the corresponding chemical reactor dynamical system

is described as [35]

$$\begin{cases} \dot{x} = \alpha_2 xy - 2\alpha_6 x^2 + (\alpha_9 - \alpha_{10})x \\ \dot{y} = -\alpha_1 xyz + \alpha_3 xy + \alpha_5 yz - 2\alpha_7 y^2 - (\alpha_{11} - \alpha_{12})y \\ \dot{z} = \alpha_1 xyz - \alpha_4 xz - \alpha_5 yz - 2\alpha_8 z^2 + \alpha_{13} z \end{cases} \tag{12}$$

where the state variables x, y and z correspond to the concentrations of species X, Y and Z respectively, α_j $(j = 1, 2, \ldots, 13)$ are positive parameters describe the relationships between reaction rates and species concentrations. When the parameters α_j $(j = 1, 2, \ldots, 13)$ are selected as in Table (1), the dynamics of the integer-order chemical reactor system (12) are chaotic. In order to enrich the study and make a contribution, we

Parameter	Value	Parameter	Value
α_1	0.88	α_8	1.333
α_2	10	α_9	999
α_3	29	α_{10}	1000
α_4	100	α_{11}	2900
α_5	100	α_{12}	100
α_6	5	α_{13}	10002.667
α_7	0.5		

Table 1. Parameter values of the fractional-order chemical reactor model (13).

extend this model to the general case of fractional-order systems. Then, the FOCRCS is described as

$$\begin{cases} {}^*D^q_{t_0} x = \alpha_2 xy - 2\alpha_6 x^2 + (\alpha_9 - \alpha_{10})x \\ {}^*D^q_{t_0} x = -\alpha_1 xyz + \alpha_3 xy + \alpha_5 yz - 2\alpha_7 y^2 - (\alpha_{11} - \alpha_{12})y \\ {}^*D^q_{t_0} x = \alpha_1 xyz - \alpha_4 xz - \alpha_5 yz - 2\alpha_8 z^2 + \alpha_{13} z \end{cases} \tag{13}$$

where x, y, z are the state variables, α_j $(j = 1, 2, \ldots, 13)$ are positive constants, and ${}^*D^q_{t_0}$ is the Caputo fractional derivative with order $q \in (0, 1]$. Applying the Adomian decomposition method described in section

(2), the numerical solution of FOCRCS (13) is given by

$$\begin{cases} x_{m+1} = \sum_{j=0}^{3} c_1^j h^{jq}/\Gamma(jq+1) \\ y_{m+1} = \sum_{j=0}^{3} c_2^j h^{jq}/\Gamma(jq+1) \\ z_{m+1} = \sum_{j=0}^{3} c_3^j h^{jq}/\Gamma(jq+1) \end{cases} \tag{14}$$

where h is iteration step size and $c_i^j (i = 1, 2, 3,\ j = 0, 1, 2, 3)$ are an intermediate variables, which can be calculated by the following formulas

$$\begin{cases} c_1^0 = x_m, \\ c_2^0 = y_m, \\ c_3^0 = z_m. \end{cases} \tag{15}$$

$$\begin{cases} c_1^1 = \alpha_2 c_1^0 c_2^0 - 2\alpha_6 (c_1^0)^2 + (\alpha_9 - \alpha_{10}) c_1^0, \\ c_2^1 = -\alpha_1 c_1^0 c_2^0 c_3^0 + \alpha_3 c_1^0 c_2^0 + \alpha_5 c_2^0 c_3^0 - 2\alpha_7 (c_2^0)^2 - (\alpha_{11} - \alpha_{12}) c_2^0, \\ c_3^1 = \alpha_1 c_1^0 c_2^0 c_3^0 - \alpha_4 c_1^0 c_3^0 - \alpha_5 c_2^0 c_3^0 - 2\alpha_8 (c_3^0)^2 + \alpha_{13} c_3^0. \end{cases} \tag{16}$$

$$\begin{cases} c_1^1 = \alpha_2 c_1^0 c_2^0 - 2\alpha_6 (c_1^0)^2 + (\alpha_9 - \alpha_{10}) c_1^0, \\ c_2^1 = -\alpha_1 c_1^0 c_2^0 c_3^0 + \alpha_3 c_1^0 c_2^0 + \alpha_5 c_2^0 c_3^0 - 2\alpha_7 (c_2^0)^2 - (\alpha_{11} - \alpha_{12}) c_2^0, \\ c_3^1 = \alpha_1 c_1^0 c_2^0 c_3^0 - \alpha_4 c_1^0 c_3^0 - \alpha_5 c_2^0 c_3^0 - 2\alpha_8 (c_3^0)^2 + \alpha_{13} c_3^0. \end{cases} \tag{17}$$

$$\begin{cases} c_1^2 = \alpha_2 (c_1^1 c_2^0 + c_1^0 c_2^1) - 4\alpha_6 (c_1^0 c_1^1) + (\alpha_9 - \alpha_{10}) c_1^1, \\ c_2^2 = -\alpha_1 (c_1^1 c_2^0 c_3^0 + c_1^0 c_2^1 c_3^0 + c_1^0 c_2^0 c_3^1) + \alpha_3 (c_1^1 c_2^0 + c_1^0 c_2^1) \\ \qquad + \alpha_5 (c_2^1 c_3^0 + c_2^0 c_3^1) - 4\alpha_7 (c_2^0 c_2^1) - (\alpha_{11} - \alpha_{12}) c_2^1, \\ c_3^2 = \alpha_1 (c_1^1 c_2^0 c_3^0 + c_1^0 c_2^1 c_3^0 + c_1^0 c_2^0 c_3^1) - \alpha_4 (c_1^1 c_3^0 + c_1^0 c_3^1) - \alpha_5 (c_2^1 c_3^0 + c_2^0 c_3^1) \\ \qquad - 4\alpha_8 (c_3^0 c_3^1) + \alpha_{13} c_3^1. \end{cases} \tag{18}$$

$$
\begin{cases}
c_1^3 = \alpha_2(c_1^2c_2^0 + \dfrac{\Gamma(2q+1)}{\Gamma^2(q+1)}c_1^1c_2^1 + c_1^0c_2^2) - 2\alpha_6(c_1^0c_1^2 \\
\quad + \dfrac{\Gamma(2q+1)}{\Gamma^2(q+1)}(c_1^1)^2) + (\alpha_9 - \alpha_{10})c_1^2, \\
c_2^3 = -\alpha_1(c_2^1c_2^0c_3^0 + c_1^0c_2^2c_3^0 + c_1^0c_2^0c_3^2 + \dfrac{\Gamma(2q+1)}{\Gamma^2(q+1)}(c_1^1c_2^1c_3^0 \\
\quad + c_1^1c_2^0c_3^1 + c_1^0c_2^1c_3^1) + \alpha_3(c_1^0c_2^2 + c_1^2c_2^0 + \dfrac{\Gamma(2q+1)}{\Gamma^2(q+1)}c_1^1c_2^1) \\
\quad + \alpha_5(c_2^0c_3^2 + c_2^2c_3^0 + \dfrac{\Gamma(2q+1)}{\Gamma^2(q+1)}c_2^1c_3^1) - 2\alpha_7(2c_2^0c_2^2 \\
\quad + \dfrac{\Gamma(2q+1)}{\Gamma^2(q+1)}(c_2^1)^2) - (\alpha_{11} - \alpha_{12})c_2^2, \\
c_3^3 = \alpha_1(c_1^2c_2^0c_3^0 + c_1^0c_2^2c_3^0 + c_1^0c_2^0c_3^2 + \dfrac{\Gamma(2q+1)}{\Gamma^2(q+1)}(c_1^1c_2^1c_3^0 + c_1^1c_2^0c_3^1 \\
\quad + c_1^0c_2^1c_3^1) - \alpha_4(c_1^0c_3^2 + c_1^2c_3^0 + \dfrac{\Gamma(2q+1)}{\Gamma^2(q+1)}c_1^1c_3^1) - \alpha_5(c_2^0c_3^2 + c_2^2c_3^0 \\
\quad + \dfrac{\Gamma(2q+1)}{\Gamma^2(q+1)}c_2^1c_3^1) - 2\alpha_8(2c_3^0c_3^2 + \dfrac{\Gamma(2q+1)}{\Gamma^2(q+1)}(c_3^1)^2) + \alpha_{13}c_3^2.
\end{cases}
\tag{19}
$$

Based on the discrete formulas in Eq.(14), the dynamical analysis of the FOCRCS (13) is investigated in the following sections.

4 Stability of equilibria

This section deals with the study of the stability of equilibrium points of the FOCRCS (13).

In fractional-order dynamical system, an equilibrium point is asymptotically stable if the following stability criterion is met [26]

$$
|\arg(\lambda(J))| > q\frac{\pi}{2}, \tag{20}
$$

where J is the Jacobian matrix of system, and $\lambda(J)$ represents the set of the eigenvalues of the matrix J. The equilibrium points of system (13) are

obtained by solving the following nonlinear equations

$$\begin{cases} \alpha_2 xy - 2\alpha_6 x^2 + (\alpha_9 - \alpha_{10})x = 0 \\ -\alpha_1 xyz + \alpha_3 xy + \alpha_5 yz - 2\alpha_7 y^2 - (\alpha_{11} - \alpha_{12})y = 0 \\ \alpha_1 xyz - \alpha_4 xz - \alpha_5 yz - 2\alpha_8 z^2 + \alpha_{13} z = 0 \end{cases} \tag{21}$$

For the parameter values listed in Table (1), and based on the stability criterion (20), the equilibrium points of system (13) and their stability are shown in Table (2).

Equilibria	Eigenvalues	Stability
$E_1 = (0, 0, 0)$	$\lambda_1 = -1, \lambda_2 = -2800, \lambda_3 = 10002.667$	unstable
$E_2 = (0, 0, 3751.94)$	$\lambda_1 = -1, \lambda_2 = 372394, \lambda_3 = -20005.34$	unstable
$E_3 = (-0.1, 0, 0)$	$\lambda_1 = 1, \lambda_2 = -2802.9, \lambda_3 = 10012.667$	unstable
$E_4 = (0, -2800, 0)$	$\lambda_1 = 0.028, \lambda_2 = -0.28, \lambda_3 = 2.9$	unstable
$E_5 = (0, 99.25, 28.99)$	$\lambda_1 = 0.9915, \lambda_{2,3} = -0.0882 \pm 5.364i$	unstable
$E_6 = (-0.1, 0, 3755.69)$	$\lambda_1 = -0.1001, \lambda_2 = 0, \lambda_3 = 3.731$	non-hyperbolic
$E_7 = (100, 100.1, 0)$	$\lambda_1 = -1.1985, \lambda_{2,3} = -0.55 \pm 1.643i$	stable
$E_8 = (73.46, 73.56, 21.02)$	$\lambda_1 = -1.3378, \lambda_{2,3} = 0.237 \pm 1.429i$	discussed

Table 2. Stability analysis of equilibria of FOCRCS (13).

Remark. For the equilibrium point $E_8 = (73.46, 73.56, 21.02)$, we have $|\arg(\lambda_1)| = \pi > q\frac{\pi}{2}$, $|\arg(\lambda_{2,3})| \approx 1.406 > q\frac{\pi}{2}$ when $q < 0.89$. Thus, the equilibrium point $E_8 = (73.46, 73.56, 21.02)$ is locally asymptotically stable if the order satisfies the condition $q \in (0, 0.89)$. However, when $q > 0.89$, the FOCRCS (13) exhibits chaotic behavior.

5 Chaotic dynamics of fractional-order chemical reactor

This section deals with the dynamical analysis of the chaotic properties of the FOCRCS (13) by employing powerful tools in nonlinear dynamic analysis.

5.1 Dynamical analysis of fractional-order chemical reactor

When the system parameters are selected as in Table (1), the initial conditions as $(x(0), y(0), z(0)) = (200, 200, 200)$, and the iteration step size h as $h = 0.00001$, the fractional-order system (13) exhibits chaotic behavior. Periodic or chaotic dynamics in 2D and 3D projections of the FOCRCS (13) for different values of fractional-order are shown in Figure (1).
Time series of states $x(t)$, $y(t)$ and $z(t)$ of the FOCRCS (13) for $q = 0.98$ are shown in Figure (2). The bifurcation diagram of the FOCRCS

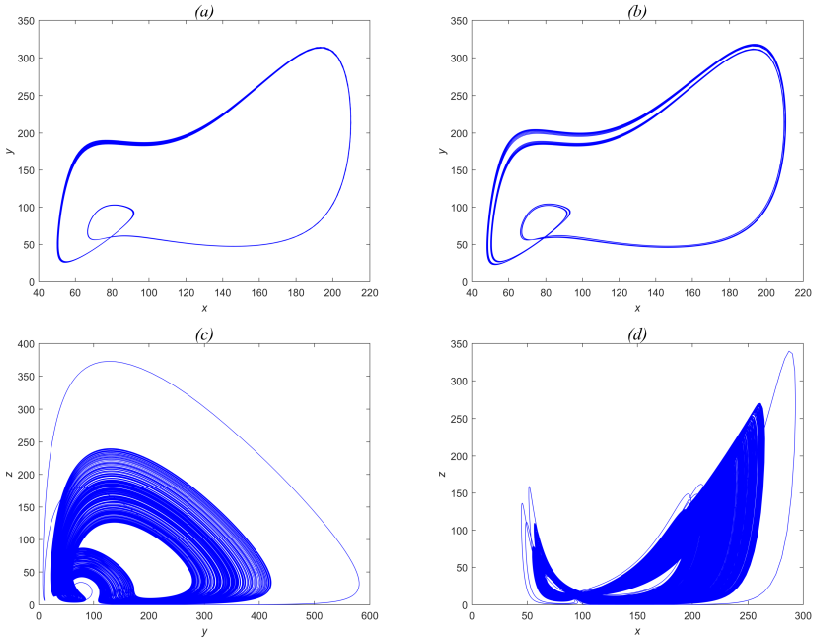

Figure 1. Chaotic attractor of the FOCRCS (13): (a) for $q = 0.891$ in $(x - y)$-plane; (b) for $q = 0.93$ in $(x - z)$-plane; (c) for $q = 0.96$ in $(y - z)$-plane; (d) for $q = 0.98$ in $(x - y - z)$-space.

(13) when the parameter α_2 ranges between $6 \leq \alpha_2 \leq 20$ is depicted in Figure (3).a. In addition, when the parameter α_3 ranges between $20 \leq \alpha_3 \leq 35$, the corresponding bifurcation diagram is represented in Figure (3).b. Clearly, the dynamic behavior of the FOCRCS (13) is influenced

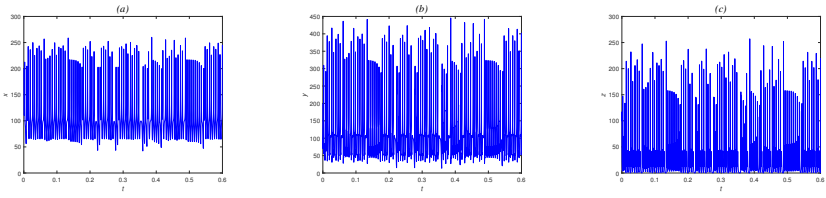

Figure 2. (a) Time series of state x; (b) Time series of state y; (c) Time series of state z.

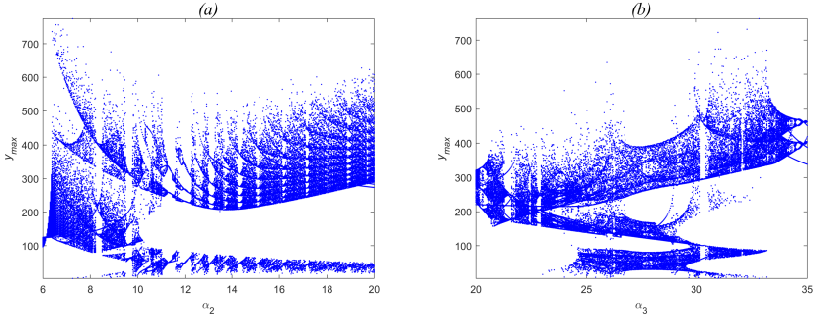

Figure 3. Bifurcation diagrams of the FOCRCS (13): (a) bifurcation diagram as α_2 varies; (b) bifurcation diagram as α_3 varies.

by the variation of its parameters. In particular, for some parameter values, the fractional-order system exhibits irregular motions, meaning that the system transitions from a stable state to a chaotic state. We can also study the influence of the fractional order on the dynamic behavior of the fractional-order system (13). Taking the same system parameters listed in Table (1), the bifurcation diagram of system (13) when the fractional order ranges between $0.891 \leq q \leq 1$ is shown in Figure (4). As one can see, a robust chaos is observed when $q \in [0.891, 1]$, then the FOCRCS (13) exhibits irregular dynamics across this derivative order q range.

In a deterministic nonlinear dynamical system, the average exponential convergence or divergence of nearby trajectories is represented by the Lyapunov exponent. The existence of a positive Lyapunov exponent is a powerful indicator of the exhibition of sensitive dependence on initial conditions, which means that the system is chaotic [39]. Using Danca MAT-

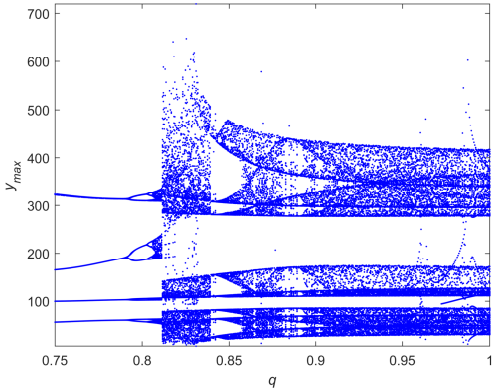

Figure 4. Bifurcation diagram of the FOCRCS (13) as q varies.

LAB code based on Benettin-Wolf algorithm to compute all Lyapunov exponents for fractional-order systems [11], for the parameter values mentioned in Table (1) and the initial state $(x(0), y(0), z(0)) = (200, 200, 200)$, Figure (5) shows the three Lyapunov exponents of the FOCRCS (13) for $q = 0.98$, which are given by

$$LE_1 = 88.5014, \qquad LE_2 = -6.25763, \qquad LE_3 = -161.669 \tag{22}$$

Since $LE_1 + LE_2 + LE_3 < 0$, the system (13) is dissipative, and the existence of attractor is confirmed. The complexity of the FOCRCS (13) is further analyzed by an estimation of the Kaplan-York fractal dimension using the following formula

$$D_{KY} = 2 + \frac{LE_1 + LE_2}{|LE_3|} \approx 2.50871 \tag{23}$$

Power spectrum analysis is a useful method for identifying chaotic behavior in nonlinear dynamical systems and can yield signal frequency information. Regular dynamics are indicated by a discrete power spectrum, while chaotic dynamics are indicated by a continuous power spectrum [28]. Figure (6) represents the normalized power spectrum density of the FOCRCS (13).

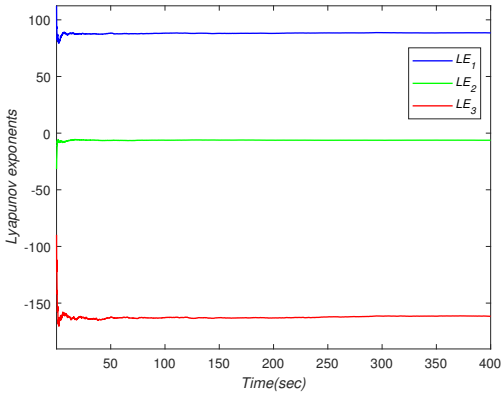

Figure 5. Lyapunov exponents spectra of the FOCRCS (13) for $q = 0.98$.

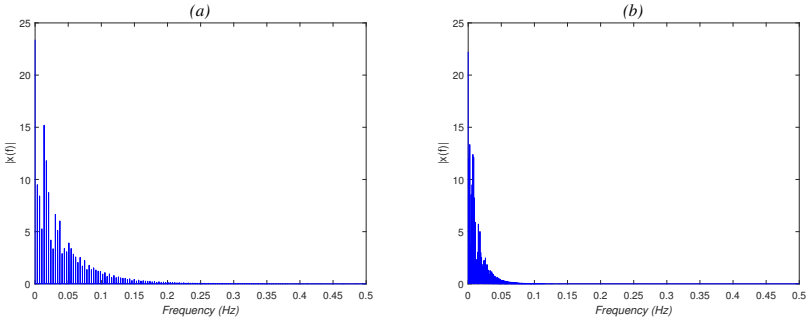

Figure 6. Normalized power spectrum density of the FOCRCS (13): (a) for $q = 0.89$; (b) for $q = 0.98$.

5.2 Complexity of the fractional-order chemical reactor system via spectral entropy

In the dynamical analysis of nonlinear chaotic systems, spectral entropy (SE) is an efficient technique that allows us to measure the level of complexity in fractional-order chaotic systems. In brief, we review the steps of algorithm which it based on Shannon definition to approximate the spectral entropy of the FOCRCS (13).

1. Based on the state x of the FOCRCS (13), we select a sequence of

data $x(i)$, $i = 0, 1, 2, \ldots, N-1$ where $N \geq 1$. SE approximation starts by deleting its current part as follows

$$x(i) = x(i) - \frac{1}{N} \sum_{s=0}^{N-1} x(s). \tag{24}$$

2. The corresponding discrete Fourier transform is given by

$$X(k) = \sum_{i=0}^{N-1} x(i) \exp[-j \frac{2\pi i k}{N}]. \tag{25}$$

where $k = 0, 1, \ldots, N-1$ and j is the imaginary unit.

3. Next, the relative power spectral density of $x(i)$ is determined as

$$p(k) = \frac{|X(k)|^2}{\sum_{k=0}^{\frac{N}{2}-1} |X(k)|^2}, \tag{26}$$

so that $\sum_{k=0}^{\frac{N}{2}-1} p(k) = 1$.

4. Then, the normalized spectral entropy is obtained by computing Shannon-entropy as follows [18]

$$SE = \frac{\sum_{k=0}^{\frac{N}{2}-1} |p(k). \ln(p(k))|}{\ln(N/2)}. \tag{27}$$

Taking the parameter values as listed in Table (1), the spectral entropy of the FOCRCS (13) with respect to fractional order is shown in Figure (7).a. As can be shown, the spectral entropy of system has higher values when the fractional order ranges between $q \in [0.891, 1]$, which means that the FOCRCS exhibits complex dynamics throughout this parameter q range. From Figure (7).b, the influence of the parameter α_3 and derivative order q on the dynamics of the FOCRCS (13) is observed when α_3 approaches 29 and $q \geq 0.891$, a higher level of complexity shown in the dynamics of the system.

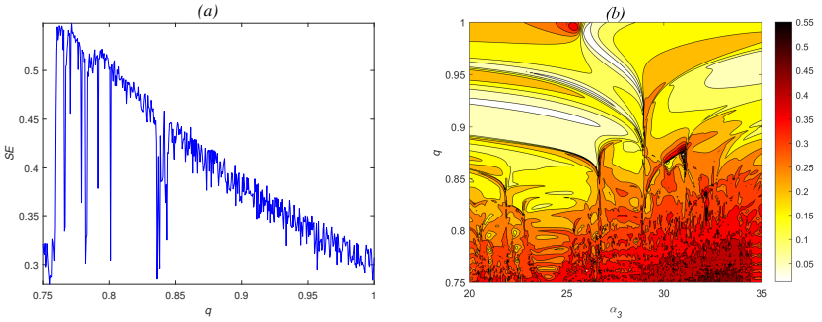

Figure 7. (a) Spectral entropy of the FOCRCS (13); (b) Chaos diagram based on SE complexity.

6 Control schemes for the fractional-order chemical reactor chaotic system

6.1 Chaos control via fractional sliding mode control

This section is devoted to the chaos control in the FOCRCS (13), where a fractional-order sliding mode controller is introduced. The main result is obtained by adopting the Lyapunov stability theory of fractional-order systems.

The controlled FOCRCS is described as

$$\begin{cases} {}^{*}D^{q}_{t_0}x = \alpha_2 xy - 2\alpha_6 x^2 + (\alpha_9 - \alpha_{10})x + \Delta H_1(x,y,z) + D_1 + u_1 \\ {}^{*}D^{q}_{t_0}y = -\alpha_1 xyz + \alpha_3 xy + \alpha_5 yz - 2\alpha_7 y^2 - (\alpha_{11} - \alpha_{12})y \\ \qquad\qquad + \Delta H_2(x,y,z) + D_2 + u_2 \\ {}^{*}D^{q}_{t_0}z = \alpha_1 xyz - \alpha_4 xz - \alpha_5 yz - 2\alpha_8 z^2 + \alpha_{13} z \\ \qquad\qquad + \Delta H_3(x,y,z) + D_3 + u_3 \end{cases} \tag{28}$$

where u_1, u_2, u_3 are the controllers for adapting the states x, y, and z of the FOCRCS (13) towards the equilibrium point (x^*, y^*, z^*). In Eq.(28), we assume that the external disturbances D_i and the uncertainties ΔH_i are both bounded, i.e $|D_i| < A_i$ and $|\Delta H_i| < B_i$ where A_i and B_i $(i = 1, 2, 3)$

are unknown positive constants. We define the control error as

$$\begin{cases} e_1 = x - x^* \\ e_2 = y - y^* \\ e_3 = z - z^* \end{cases} \tag{29}$$

Differentiating Eq.(29), the fractional-order error system can be obtained as

$$\begin{cases} {}^*D^q e_1 = \alpha_2(e_1 + x^*)(e_2 + y^*) - 2\alpha_6(e_1 + x^*)^2 \\ \qquad + (\alpha_9 - \alpha_{10})(e_1 + x^*) + \Delta H_1(x, y, z) + D_1 + u_1 \\ {}^*D^q e_2 = -\alpha_1(e_1 + x^*)(e_2 + y^*)(e_3 + z^*) + \alpha_3(e_1 + x^*)(e_2 + y^*) \\ \qquad + \alpha_5(e_2 + y^*)(e_3 + z^*) - 2\alpha_7(e_2 + y^*)^2 \\ \qquad - (\alpha_{11} - \alpha_{12})(e_2 + y^*) + \Delta H_2(x, y, z) + D_2 + u_2 \\ {}^*D^q e_3 = \alpha_1(e_1 + x^*)(e_2 + y^*)(e_3 + z^*) - \alpha_4(e_1 + x^*)(e_3 + z^*) \\ \qquad - \alpha_5(e_2 + y^*)(e_3 + z^*) - 2\alpha_8(e_3 + z^*)^2 + \alpha_{13}(e_3 + z^*) \\ \qquad + \Delta H_3(x, y, z) + D_3 + u_3 \end{cases} \tag{30}$$

Next, we define the sliding surface in the control error space as

$$s_i(t) = {}^*D^{q-1} e_i(t) + \lambda_i \int_0^t e_i(\tau) d\tau, \tag{31}$$

where $\lambda_i > 0$ is the sliding speed for $i = 1, 2, 3$.
In order to make Eq.(31) operate in sliding mode, we set the following condition

$$s_i(t) = 0, \quad \dot{s}_i(t) = 0 \quad \text{for } i = 1, 2, 3. \tag{32}$$

The fractional derivative of Eq.(31) is obtained as

$$\dot{s}_i(t) = {}^*D^q e_i(t) + \lambda_i e_i(t), \ i = 1, 2, 3. \tag{33}$$

Using Eq.(32)-Eq.(33), we obtain

$${}^*D^q e_i = -\lambda_i e_i(t), \ i = 1, 2, 3. \tag{34}$$

Since $\lambda_i > 0$ $(i = 1, 2, 3)$, according to the Lyapunov stability theory of fractional-order systems, the fractional-order error system (34) is asymptotically stable.

Based on Eq.(30)-Eq.(34) and adopting the sliding mode control theory, the control laws can be designed as

$$\begin{cases} u_1 = -\alpha_2 xy + 2\alpha_6 x^2 - (\alpha_9 - \alpha_{10})x - \lambda_1 e_1 - (\hat{A}_1 + \hat{B}_1 + k_1)\text{sign}(s_1) \\ u_2 = \alpha_1 xyz - \alpha_3 xy - \alpha_5 yz + 2\alpha_7 y^2 + (\alpha_{11} - \alpha_{12})y - \lambda_2 e_2 \\ \qquad - (\hat{A}_2 + \hat{B}_2 + k_2)\text{sign}(s_2) \\ u_3 = -\alpha_1 xyz + \alpha_4 xz + \alpha_5 yz + 2\alpha_8 z^2 - \alpha_{13} z - \lambda_3 e_3 \\ \qquad - (\hat{A}_3 + \hat{B}_3 + k_3)\text{sign}(s_3) \end{cases} \tag{35}$$

where $k_i > 0$ for $i = 1, 2, 3$ are gain constants.

We select the adaptive parameter update law as

$$\begin{cases} \dot{\hat{A}}_i = \eta_i |s_i|, \quad i = 1, 2, 3. \\ \dot{\hat{B}}_i = \gamma_i |s_i|, \quad i = 1, 2, 3. \end{cases} \tag{36}$$

where $\eta_i > 0$, $\gamma_i > 0$ for $i = 1, 2, 3$. The next result is obtained by employing the Lyapunov stability theory [40].

Theorem 1. *The FOCRCS with uncertainties and disturbances is rendered globally asymptotically stable around the equilibrium point* (x^*, y^*, z^*) *for all initial conditions using control and update laws given in* (35)-(36).

Proof. Consider the candidate Lyapunov function defined on $\mathbb{R}^9$ by

$$V = V_1 + V_2 + V_3, \tag{37}$$

where

$$\begin{cases} V_1 = \frac{1}{2}s_1^2 + \frac{1}{2\eta_1}(\hat{A}_1 - A_1)^2 + \frac{1}{2\gamma_1}(\hat{B}_1 - B_1)^2 \\ V_2 = \frac{1}{2}s_2^2 + \frac{1}{2\eta_2}(\hat{A}_2 - A_2)^2 + \frac{1}{2\gamma_2}(\hat{B}_2 - B_2)^2 \\ V_3 = \frac{1}{2}s_3^2 + \frac{1}{2\eta_3}(\hat{A}_3 - A_3)^2 + \frac{1}{2\gamma_3}(\hat{B}_3 - B_3)^2 \end{cases} \tag{38}$$

Thus, the time derivative of Eq.(38) is given by

$$\begin{cases} \dot{V}_1 = s_1\dot{s}_1 + \frac{1}{\eta_1}(\hat{A}_1 - A_1)\dot{\hat{A}}_1 + \frac{1}{\gamma_1}(\hat{B}_1 - B_1)\dot{\hat{B}}_1 \\ \dot{V}_2 = s_2\dot{s}_2 + \frac{1}{\eta_2}(\hat{A}_2 - A_2)\dot{\hat{A}}_2 + \frac{1}{\gamma_2}(\hat{B}_2 - B_2)\dot{\hat{B}}_2 \\ \dot{V}_3 = s_3\dot{s}_3 + \frac{1}{\eta_3}(\hat{A}_3 - A_3)\dot{\hat{A}}_3 + \frac{1}{\gamma_3}(\hat{B}_3 - B_3)\dot{\hat{B}}_3 \end{cases} \tag{39}$$

From Eq.(33), we have

$$\begin{cases} \dot{V}_1 = s_1({}^*D^q e_1 + \lambda_1 e_1) + \frac{1}{\eta_1}(\hat{A}_1 - A_1)\dot{\hat{A}}_1 + \frac{1}{\gamma_1}(\hat{B}_1 - B_1)\dot{\hat{B}}_1 \\ \dot{V}_2 = s_2({}^*D^q e_2 + \lambda_2 e_2) + \frac{1}{\eta_2}(\hat{A}_2 - A_2)\dot{\hat{A}}_2 + \frac{1}{\gamma_2}(\hat{B}_2 - B_2)\dot{\hat{B}}_2 \\ \dot{V}_3 = s_3({}^*D^q e_3 + \lambda_3 e_3) + \frac{1}{\eta_3}(\hat{A}_3 - A_3)\dot{\hat{A}}_3 + \frac{1}{\gamma_3}(\hat{B}_3 - B_3)\dot{\hat{B}}_3 \end{cases} \tag{40}$$

Substituting Eq.(30), Eq.(35) and Eq.(36) into Eq.(40), we obtain

$$\begin{cases} \dot{V}_i = s_i[(\Delta H_i + D_i) - (\hat{A}_i + \hat{B}_i + k_i)\text{sign}(s_i)] + (\hat{A}_i - A_i)|s_i| \\ \quad + (\hat{B}_i - B_i)|s_i| \\ \quad \leq (|\Delta H_i| + |D_i|)|s_i| - (\hat{A}_i + \hat{B}_i + k_i)|s_i| + (\hat{A}_i - A_i)|s_i| \\ \quad + (\hat{B}_i - B_i)|s_i| \\ \quad < (A_i + B_i)|s_i| - (\hat{A}_i + \hat{B}_i + k_i)|s_i| + (\hat{A}_i - A_i)|s_i| + (\hat{B}_i - B_i)|s_i| \\ \quad = -k_i|s_i|, \quad i = 1, 2, 3. \end{cases} \tag{41}$$

Therefore, we get

$$\dot{V} = \sum_{i=1}^{3} \dot{V}_i < -\sum_{i=1}^{3} k_i|s_i|. \tag{42}$$

Hence, $\dot{V}$ is negative-definite. Using Barbalat's lemma [14], it is deduced that the fractional-order errors asymptotically converge to $s_i = 0$ for $i = 1, 2, 3$. Therefore, the state trajectories of the FOCRCS with uncertainties and external disturbances are globally and asymptotically stable around the equilibrium point (x^*, y^*, z^*) for all initial conditions. ■

6.1.1 Numerical simulations

For numerical simulations, the system parameters are selected as listed in Table (1), the fractional order is selected as $q = 0.98$. The initial state

of the FOCRCS is chosen as $(x(0), y(0), z(0)) = (200, 200, 200)$. Also, we select $\lambda_i = 15\,(i = 1, 2, 3)$, and the gain parameters as $k_i = 20\,(i = 1, 2, 3)$. The gains of the adaptive law are taken as $\eta_i = 1.25$, $\gamma_i = 1.25$ for $i = 1, 2, 3$. We take $D_1 = 4\cos(\pi t)$, $D_2 = -\cos(\pi(t - 0.2))$, $D_3 = 2\sin(\pi(t - 0.4))$, and $\Delta H_1(x, y, z) = \cos(\pi(x + y + z))$, $\Delta H_2(x, y, z) = \sin(z - y)$, $\Delta H_3(x, y, z) = \cos(y+z)$. The evolution of controlled states $x(t)$, $y(t)$, and $z(t)$ around the equilibrium point $E_5 = (0, 99.25, 28.99)$ is displayed in Figure (8).a, whereas the control errors $e_1(t)$, $e_2(t)$ and $e_3(t)$ are shown in Figure (8).b. To show again the robustness of the constructed control scheme,

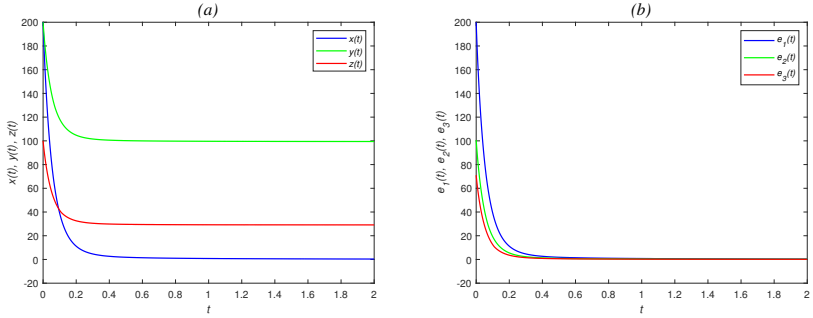

Figure 8. (a) Evolution of the controlled states $x(t)$, $y(t)$, and $z(t)$ for $q = 0.98$; (b) Time-history of the control errors $e_1(t)$, $e_2(t)$, and $e_3(t)$.

the initial conditions are selected as $(x(0), y(0), z(0)) = (200, 100, 200)$. The evolution of controlled states $x(t)$, $y(t)$, and $z(t)$ around the equilibrium point $E_8 = (73.46, 73.56, 21.02)$ is shown in Figure (9).a, while the control errors $e_1(t)$, $e_2(t)$, and $e_3(t)$ are depicted in Figure (9).b. Obviously, in two previous cases, the control errors converge towards zero asymptotically in sufficient time, which shows the feasibility of the control method.

6.2 Chaos synchronization of fractional-order chemical reactor chaotic systems

In this part, we construct a synchronization scheme between two identical fractional-order chemical reactor chaotic systems. The drive system is

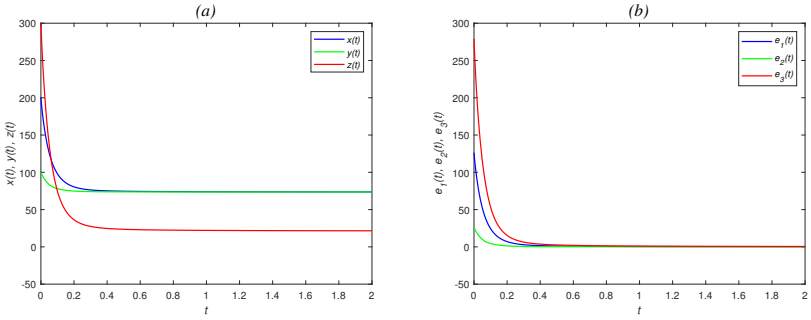

Figure 9. (a) Evolution of the controlled states $x(t)$, $y(t)$, and $z(t)$ for $q = 0.98$; (b) Time-history of the control errors $e_1(t)$, $e_2(t)$, and $e_3(t)$.

given by

$$\begin{cases} {}^{*}D^{q}_{t_0} x_1 = \alpha_2 x_1 y_1 - 2\alpha_6 x_1^2 + (\alpha_9 - \alpha_{10}) x_1 \\ {}^{*}D^{q}_{t_0} y_1 = -\alpha_1 x_1 y_1 z_1 + \alpha_3 x_1 y_1 + \alpha_5 y_1 z_1 - 2\alpha_7 y_1^2 - (\alpha_{11} - \alpha_{12}) y_1 \\ {}^{*}D^{q}_{t_0} z_1 = \alpha_1 x_1 y_1 z_1 - \alpha_4 x_1 z_1 - \alpha_5 y_1 z_1 - 2\alpha_8 z_1^2 + \alpha_{13} z_1 \end{cases} \tag{43}$$

while the response system can be expressed as

$$\begin{cases} {}^{*}D^{q}_{t_0} x_2 = \alpha_2 x_2 y_2 - 2\alpha_6 x_2^2 + (\alpha_9 - \alpha_{10}) x_2 + u_1(t) \\ {}^{*}D^{q}_{t_0} y_2 = -\alpha_1 x_2 y_2 z_2 + \alpha_3 x_2 y_2 + \alpha_5 y_2 z_2 - 2\alpha_7 y_2^2 \\ \qquad\qquad - (\alpha_{11} - \alpha_{12}) y_2 + u_2(t) \\ {}^{*}D^{q}_{t_0} z_2 = \alpha_1 x_2 y_2 z_2 - \alpha_4 x_2 z_2 - \alpha_5 y_2 z_2 - 2\alpha_8 z_2^2 + \alpha_{13} z_2 + u_3(t) \end{cases} \tag{44}$$

where $u_i(t)$ $(i = 1, 2, 3)$ are the control functions to be designed.
The synchronization error is defined as

$$\begin{cases} e_1 = x_2 - x_1 \\ e_2 = y_2 - y_1 \\ e_3 = z_2 - z_1 \end{cases} \tag{45}$$

Using Eq.(43) and Eq.(44), the fractional-order error system is given as

$$\begin{cases} {}^{*}D_{t_0}^{q} e_1 = \alpha_2(x_2y_2 - x_1y_1) - 2\alpha_6(x_2^2 - x_1^2) + (\alpha_9 - \alpha_{10})e_1 + u_1(t) \\ {}^{*}D_{t_0}^{q} e_2 = -\alpha_1(x_2y_2z_2 - x_1y_1z_1) + \alpha_3(x_2y_2 - x_1y_1) \\ \qquad + \alpha_5(y_2z_2 - y_1z_1) - 2\alpha_7(y_2^2 - y_1^2) - (\alpha_{11} - \alpha_{12})e_2 + u_2(t) \\ {}^{*}D_{t_0}^{q} e_3 = \alpha_1(x_2y_2z_2 - x_1y_1z_1) - \alpha_4(x_2z_2 - x_1z_1) - \alpha_5(y_2z_2 - y_1z_1) \\ \qquad - 2\alpha_8(z_2^2 - z_1^2) + \alpha_{13}e_3 + u_3(t) \end{cases} \tag{46}$$

Then, we take the activation feedback control functions as

$$\begin{cases} u_1(t) = -\alpha_2(x_2y_2 - x_1y_1) + 2\alpha_6(x_2^2 - x_1^2) + v_1(t) \\ u_2(t) = \alpha_1(x_2y_2z_2 - x_1y_1z_1) - \alpha_3(x_2y_2 - x_1y_1) - \alpha_5(y_2z_2 - y_1z_1) \\ \qquad + 2\alpha_7(y_2^2 - y_1^2) + v_2(t) \\ u_3(t) = -\alpha_1(x_2y_2z_2 - x_1y_1z_1) + \alpha_4(x_2z_2 - x_1z_1) + \alpha_5(y_2z_2 - y_1z_1) \\ \qquad + 2\alpha_8(z_2^2 - z_1^2) + v_3(t) \end{cases} \tag{47}$$

where $v_i(t)$ $(i = 1, 2, 3)$ are the control inputs, which are selected as

$$\begin{bmatrix} v_1(t) \\ v_2(t) \\ v_3(t) \end{bmatrix} = M \begin{bmatrix} e_1 \\ e_2 \\ e_3 \end{bmatrix} \tag{48}$$

where M is a 3×3 constant matrix selected as

$$M = \begin{pmatrix} \alpha_{10} - \alpha_9 - 1 & 0 & 0 \\ -1 & \alpha_{11} - \alpha_{12} - 1 & 0 \\ 0 & 0 & -(\alpha_{13} + 1) \end{pmatrix} \tag{49}$$

Hence, the fractional-order error system is obtained as

$$\begin{cases} {}^{*}D_{t_0}^{q} e_1 = -e_1 \\ {}^{*}D_{t_0}^{q} e_2 = -e_1 - e_2 \\ {}^{*}D_{t_0}^{q} e_3 = -e_3 \end{cases} \tag{50}$$

which can be expressed in matrix form as

$$\left({}^{*}D^{q}e_1, {}^{*}D^{q}e_2, {}^{*}D^{q}e_3\right)^{T} = N \times \left(e_1, e_2, e_3\right)^{T}, \tag{51}$$

where

$$N = \begin{pmatrix} -1 & 0 & 0 \\ -1 & -1 & 0 \\ 0 & 0 & -1 \end{pmatrix} \tag{52}$$

Since all the eigenvalues $\lambda_i = -1$ $(i = 1, 2, 3)$ of matrix N, the stability condition $|\arg(\lambda_i)| > q\frac{\pi}{2}$ $(i = 1, 2, 3)$ is met. According to the Lyapunov stability theory of the fractional-order systems, the fractional-order error system (50) is asymptotically stable. Hence, the fractional-order drive and response systems (43) and (44) can achieve asymptotic synchronization.

6.2.1 Numerical simulations

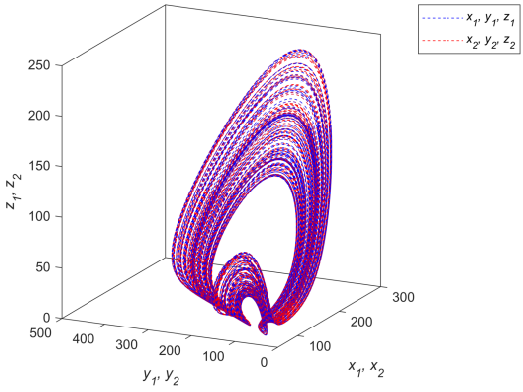

Figure 10. The synchronized chaotic attractors of the drive and response fractional-order chemical reactor systems for $q = 0.98$ in (x, y)-plane.

For numerical simulations, the parameter values are selected as mentioned in Table (1), and the fractional order is taken as $q = 0.98$. The initial state of the drive and response systems are taken as $(x_1(0), y_1(0), z_1(0)) = (400, 100, 100)$ and

$(x_2(0), y_2(0), z_2(0)) = (280, 190, 140)$, respectively. Figure (10) represents the synchronized attractors of the drive and response systems. The time evolution of states of systems (43) and (44) is shown in Figure (11). Figure

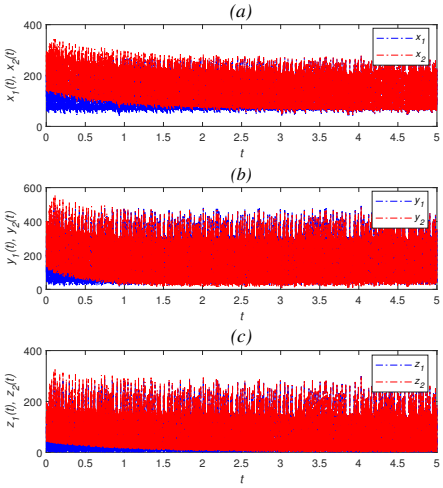

Figure 11. Synchronization between the state variables of the drive system (43) and the state variables of the response system (44): (a) x_1 and x_2; (b) y_1 and y_2; (c) z_1 and z_2.

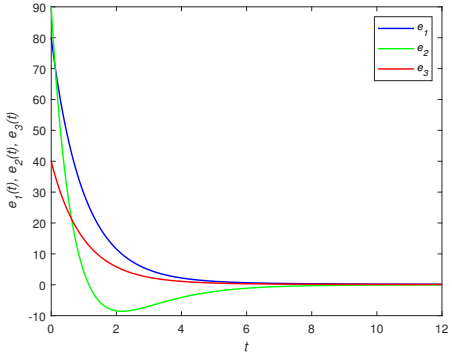

Figure 12. Time-history of the synchronization errors e_1, e_2, e_3.

(12) displays the time-history of the synchronization error $e = (e_1, e_2, e_3)^T$. As we can see, the error tends to zero as $t \to \infty$, this shows the accuracy of the constructed synchronization scheme.

7 Conclusion

Two main goals were derived from this research paper. The first is to conduct a descriptive and numerical study of the chaotic behavior of a FOCRCS by means of powerful tools in nonlinear dynamic analysis such as phase plots, bifurcation diagrams, and chaos diagrams. Moreover, the spectral entropy based on the Shannon definition has been computed in order to measure the level of complexity in the FOCRCS. The second goal is to control the chaotic dynamics in the studied model via an adaptive sliding mode control strategy. In addition, chaos synchronization was achieved between two identical non-integer chemical reactor systems by adopting an active control method. Numerical simulations in MATLAB were implemented to validate the theoretical results obtained in this study.

The last mutation in fractional calculus theorems allows us to study physical and chemical systems by employing new fractional derivatives in order to understand the evolution of real-world phenomena in nature, physics, chemistry, and engineering.

***Acknowledgment*:** The authors like to express their gratitude to everyone who helped to complete this research work.

References

[1] G. Adomian, A review of the decomposition method and some recent results for nonlinear equations, *Math. Comput. Model.* **13** (1990) 17–43.

[2] E. Ahmed, A. Hashish, F. A. Rihan, On fractional order cancer model, *Fract. Calc. Appl. Anal.* **3** (2012) 1–6.

[3] C. Baishya, R. N. Premakumari, M. E. Samei, M. K. Naik, Chaos control of fractional order nonlinear Bloch equation by utilizing sliding mode controller, *Chaos Solitons & Fractals* **174** (2023) #113773.

[4] S. Bekiros, Q. Yao, J. Mou, A. F. Alkhateeb, H. Jahanshahi, Adaptive fixed-time robust control for function projective synchronization of hyperchaotic economic systems with external perturbations, *Chaos Solitons & Fractals* **172** (2023) #113609.

[5] I. Bodale, V. A. Oancea, Chaos control for Willamowski-Rössler model of chemical reactions, *Chaos Solitons & Fractals* **78** (2015) 1–9.

[6] A. Buscarino, C. Famoso, L. Fortuna, M. Frasca, A new chaotic electro-mechanical oscillator, *Int. J. Bifurc. Chaos Appl. Sci. Eng.* **26** (2016) #1650161.

[7] D. Cafagna, G. Grassi, Bifurcation and chaos in the fractional-order Chen system via a time-domain approach, *Int. J. Bifurc. Chaos Appl. Sci. Eng.* **18** (2008) 1845–1863.

[8] D. Cafagna, G. Grassi, Hyperchaos in the fractional-order Rössler system with lowest-order, *Int. J. Bifurc. Chaos Appl. Sci. Eng.* **19** (2009) 339–347.

[9] M. Caputo, M. Fabrizio, A new definition of fractional derivative without singular kernel, *Prog. Fract. Differ. Appl.* **1** (2015) 73–85.

[10] A. Charef, H. H. Sun, Y. Y. Tsao, B. Onaral, Fractal system as represented by singularity function, *IEEE Trans. Autom. Control.* **37** (1992) 1465–1470.

[11] M. F. Danca, N. Kuznetsov, Matlab code for Lyapunov exponents of fractional-order systems, *Int. J. Bifurc. Chaos Appl. Sci. Eng.* **28** (2018) #1850067.

[12] R. Devaney, *An Introduction to Chaotic Dynamical Systems*, CRC Press, London, 2018, pp. 48–52.

[13] Y. P. Dousseh, A. V. Monwanou, A. A. Koukpémèdji, C. H. Miwadinou, J. B. Chabi Orou, Dynamics analysis, adaptive control, synchronization and anti-synchronization of a novel modified chaotic financial system, *Int. J. Dyn. Contr.* **11** (2023) 862–876.

[14] J. A. Gallegos, M. A. Duarte-Mermoud, N. Aguila-Camacho, R. Castro-Linares, On fractional extensions of Barbalat lemma, *Syst. Control Lett.* **84** (2015) 7–12.

[15] C. Goodrich, A. C. Peterson, *Discrete Fractional Calculus*, Springer, Berlin, 2015, pp. 87–117.

[16] R. Gorenflo, F. Mainardi, *Fractional Calculus: Integral and Differential Equations of Fractional Order*, Springer, Vienna, 1997, pp. 223–276.

[17] N. Haneche, T. Hamaizia, A secure communication scheme based on generalized modified projective synchronization of a new 4-D fractional-order hyperchaotic system, *Phys. Scr.* **99** (2024) #095203.

[18] S. He, K. Sun, H. Wang, Complexity analysis and DSP implementation of the fractional-order Lorenz hyperchaotic system, *Entropy* **17** (2015) 8299–8311.

[19] E. Kaslik, S. Sivasundaram, Dynamical analysis and chaos control of the fractional chaotic ecological model, *Neural Networks* **32** (2012) 245–256.

[20] H. Kheiri, B. Naderi, Dynamical behavior and synchronization of chaotic chemical reactors model, *Iranian J. Math. Chem.* **6** (2015) 81–92.

[21] A. A. Khennaoui, A. Ouannas, S. Bendoukha, X. Wang, V. T. Pham, On chaos in the fractional-order discrete-time unified system and its control synchronization, *Entropy* **20** (2018) #530.

[22] A. A. Kilbas, H. M. Srivastava, J. J. Trujillo, *Theory and Applications of Fractional Differential Equations*, Elsevier, Amsterdam, 2006, pp. 69–99.

[23] S. Kumari, M. Dua, S. Dua, D. Dhingra, A novel Cosine-Cosine chaotic map-based video encryption scheme, *J. Eng. Appl. Sci.* **71** (2024) #36.

[24] E. E. Mahmoud, P. Trikha, L. S. Jahanzaib, O. A. Almaghrabi, Dynamical analysis and chaos control of the fractional chaotic ecological model, *Chaos Solitons & Fractals* **141** (2020) #110348.

[25] M. Marwan, A. Xiong, M. Han, R. Khan, Chaotic behavior of Lorenz-based chemical system under the influence of fractals, *MATCH Commun. Math. Comput. Chem.* **91** (2024) 307-336.

[26] D. Matignon, Stability results for fractional differential equations with applications to control processing, *Comput. Engin. Sys. Appl.* **2** (1996) 963–968.

[27] A. E. Matouk, B. Lahcene, Chaotic dynamics in some fractional predator-prey models via a new Caputo operator based on the generalised Gamma function, *Chaos Solitons & Fractals* **166** (2023) #112946.

[28] I. Melbourne, G. A. Gottwald, Power spectra for deterministic chaotic dynamical systems, *Nonlinearity* **21** (2007) #179.

[29] I. Podlubny, *Fractional Differential Equations : An Introduction to Fractional Derivatives, Fractional Differential Equations, to Methods of Their Solution and Some of Their Applications*, Academic Press, San Diego, 1999, pp. 41–119.

[30] R. Ramamoorthy, K. Rajagopal, G. D. Leutcho, O. Krejcar, H. Namazi, I. Hussain, Multistable dynamics and control of a new 4D memristive chaotic Sprott B system, *Chaos Solitons & Fractals* **156** (2022) #111834.

[31] R. Robertson, A. Combs, *Chaos Theory in Psychology and the Life Sciences*, Taylor & Francis, United Kingdom, 2014, pp. 253–295.

[32] S. G. Samko, A. A. Kilbas, O. I. Marichev, *Fractional Integrals and Derivatives. Theory and Applications*, Gordon & Breach, Amsterdam, 1993, pp. 28–46.

[33] F. Setoudeh, M. M. Dezhdar, M. Najafi, Nonlinear analysis and chaos synchronization of a memristive-based chaotic system using adaptive control technique in noisy environments, *Chaos Solitons & Fractals* **164** (2022) #112710.

[34] N. T. Shawagfeh, Analytical approximate solutions for nonlinear fractional differential equations, *Appl. Math. Comput.* **131** (2002) 517–529.

[35] P. P. Singh, B. K. Roy, Microscopic chaos control of chemical reactor system using nonlinear active plus proportional integral sliding mode control technique, *Eur. Phys. J.* **228** (2019) 169–184.

[36] S. H. Strogatz, *Nonlinear Dynamics and Chaos: With Applications to Physics, Biology, Chemistry, and Engineering*, CRC Press, London, 2018, pp. 335–370.

[37] H. H. Sun, A. Abdelwahab, B. Onaral, Linear approximation of transfer function with a pole of fractional power, *IEEE Trans. Autom. Control.* **29** (1984) 441–444.

[38] A. Uchida, F. Rogister, J. Garcia-Ojalvo, R. Roy, Synchronization and communication with chaotic laser systems, *Prog. Opt.* **48** (2005) 203–341.

[39] S. Vaidyanathan, A. T. Azar, *Analysis and Control of a 4-D Novel Hyperchaotic System*, Springer, Cham, 2015, pp. 3–17.

[40] Z. Vukić, L. Kuljača, D. Djonlagić, S. Tešnjak, *Nonlinear Control Systems*, CRC Press, Boca Raton, 2003, pp. 56–100.

[41] S. Wang, A novel memristive chaotic system and its adaptive sliding mode synchronization, *Chaos Solitons & Fractals* **172** (2023) #113533.

[42] Z. Wang, A. J. M. Khalaf, S. Jafari, S. Panahi, C. Li, I. Hussain, A new memristive chaotic system with a plane and two lines of equilibria, *Int. J. Bifurc. Chaos Appl. Sci. Eng.* **31** (2021) #2150066.

[43] H. Wang, Q. S. Li, Microscopic dynamics of deterministic chemical chaos, *J. Phys. Chem. A* **104** (2000) 472–475.

[44] H. H. Wang, K. H. Sun, S. B. He, Dynamic analysis and implementation of a digital signal processor of a fractional-order Lorenz-Stenflo system based on the Adomian decomposition method, *Phys. Scr.* **90** (2014) #015206.

[45] T. Wang, Y. Zhang, Y. Che, Chaos control and synchronization of two neurons exposed to elf external electric field, *Chaos Solitons & Fractals* **34** (2007) 839–850.

[46] X. Wu, Z. Fu, J. Kurths, A secure communication scheme based generalized function projective synchronization of a new 5D hyperchaotic system, *Phys. Scr.* **90** (2015) #045210.

[47] X. Wu, H. Shi, M. Ji'e, S. Duan, L. Wang, A novel image compression and encryption scheme based on conservative chaotic system and DNA method, *Chaos Solitons & Fractals* **172** (2023) #113492.

[48] X. J. Wu, H. Wang, H. T. Lu, Hyperchaotic secure communication via generalized function projective synchronization, *Nonlin. Anal. Real World Appl.* **12** (2011) 1288–1299.

[49] Z. J. Xin, Q. Lai, Dynamical investigation and encryption application of a new multiscroll memristive chaotic system with rich offset boosting features, *Chaos Solitons & Fractals* **181** (2024) #114696.

[50] C. Xu, Y. Wu, Bifurcation and control of chaos in a chemical system, *Appl. Math. Model.* **39** (2015) 2295–2310.

[51] M. T. Yassen, Chaos synchronization between two different chaotic systems using active control, *Chaos Solitons & Fractals* **23** (2005) 131–140.

[52] Y. Zhang, H. Xiang, S. Zhang, L. Liu, Construction of high-dimensional cyclic symmetric chaotic map with one- dimensional chaotic map and its security application, *Multimed. Tools Appl.* **82** (2023) 17715–17740.